Original Paper

Mechanisms of the formation of gas bubbles in heat treatment of glass-silicate tiles

Jurij Linhart

Progressive Technologies s.r.o., Prague (Czech Republic)

Theoretical research has been done into the mechanisms of the formation of gas bubbles which takes place during the sintering of the glass granulation product under the conditions of heating its upper layer. It is shown that in the bubble, there is a possibility of an inverse thermal distribution which will lead to a thermal jump on its boundary. At the thermal processing temperatures, the presence of CO_2 increases the effect of absorption of the radiation conditioned by the spectral zones. Experimentally, it has been proved that a thermal field inversion takes place in the presence of an inner diffusing layer joined to a clearly transparent one for the thermal radiation of the material.

1. Introduction

The technologies and plants for the production of glass-silicate tiles developed in the last few years make it possible to effectively use glass industry wastes and various silicate materials for producing decorative lining tiles for indoor and outdoor use which imitate expensive natural materials such as granite, marble or malachite among others. This new composite material has been named glass-silicate [1 and 2].

The technological process consists of preparing glass industry wastes in the form of powders of certain granulometric composition, pouring these powders into heat-resistant moulds with subsequent thermal processing in a furnace where the semi-finished product is subjected to successive heating phases. Then the upper layer is slightly melted and the bottom layer is sintered, and subsequently the resulting product is annealed and cooled down to room temperature.

The maximum temperature during thermal processing is up to 1000 to 1100 °C on the surface and 850 to 950 °C in the bottom layers where the sintering of the original raw material takes place. One of the problems in making high-quality products with high-strength properties is that gas bubbles form in the inner layers of the semi-finished product during thermal processing and rise to the surface.

The purpose of this work was to carry out a detailed analysis of the causes of the formation of gas bubbles in thermal processing of glass-silicate semi-finished products. Several mechanisms of the formation of gas bubbles have been dealt with and there has been shown their inseparable connection with the specific problem of the formation of a thermal field in the bubble where local overheated areas originate inside the layer of the material. The results may also be of interest to the experts in the field of repeated processing of glass.

Received 9 August, revised manuscript 3 December 2001.

2. Theoretical part

2.1 Technological conditions of the process

The analysis of the composition of gases found in the cavities in different layers of the finished product showed that it is chiefly made up of air and CO_2 as well as, in a much lower amount, of CO and SO_2. Therefore it is obvious that the bubbles form not only out of the air mechanically brought into the semi-finished product. They also form due to a decomposition of the remnants of carbonates and sulphates and as a consequence of a possible penetration of smaller particles of the fire-resistant material, organic mixtures, iron, etc. into the poured-in material. It also follows that the mechanisms of the formation of the pores must be different.

It has been established that there are four most probably and frequently occurring mechanisms of gas bubble formation taking place during thermal processing of a silicate semi-finished product. We will deal with these mechanisms one by one.

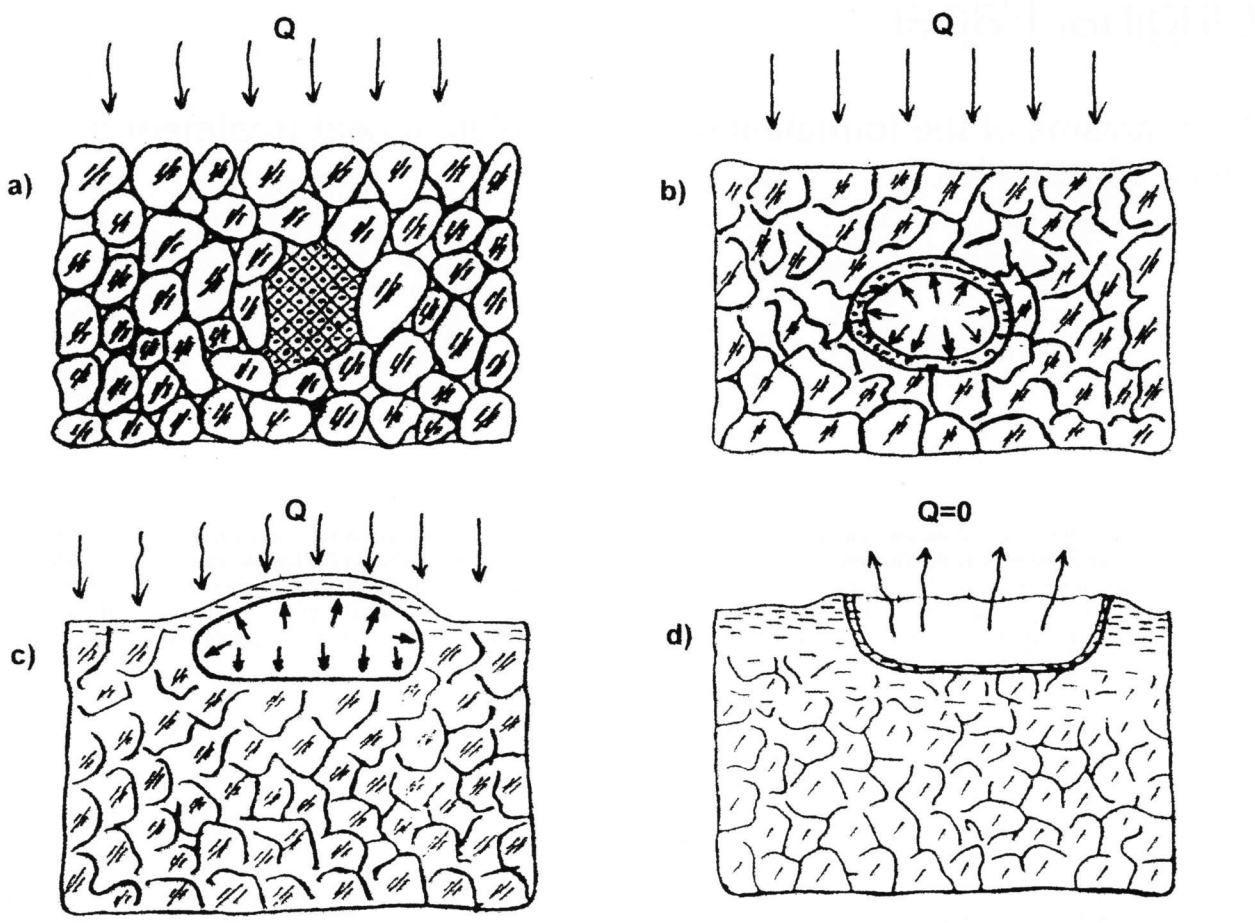

Figures 1a to d. Various stages of formation and floating of a gas bubble arising at the agglomeration point of glass dust particles (Q = heat flux); a) formation of the powder-like glass particles region inside of glass granulate, b) melting of powder-like glass particles and formation of bubble with a semitransparent diffuse spectral membrane inside of glass granulate layer, c) gas bubble growth with a movement towards the surface, d) cavity formation on the surface after burst of gas bubble.

In the production of single-layer slabs where only glass granulate is used without any other materials being added, dust particles can gather at individual points inside the glass (figure 1a), after the granule is poured in the mould and after vibration sealing is carried out. The occurrence of local gatherings of glass dust is particularly probable if the glass granulation product is prepared by way of mechanical grinding and if vibration sealing is used for the poured-in material. In this case, the glass dust penetrates into sufficiently big cavities in the middle and bottom layers of the basic glass product whose granules are of a size of 1 to 3 mm and make up 85 to 90 % of the total volume. If the method of water granulation by way of thermal stroke is used for the preparation of the source raw material where the particles of a size smaller than 0.2 mm are absent, the possibility of similar gatherings is almost ruled out.

As the temperature is increased, the gas (usually air) found at the point of a dust gathering starts to expand and pushes the smallest glass particles in all directions. Thus it forms a cavity inside the granulate (figure 1b) whose boundary consists of an unbroken surface of the sealed glass particles with the layer being approximately 0.1 to 0.2 mm thick and the size of the negligible particles being 0.05 mm.

In the process of further heating, the bubbles thus formed rise to the surface (figure 1c) and if the viscosity of the upper layer is sufficiently low, then the surface is broken and a crater forms (figure 1d).

The starting point for the sintering and the subsequent melting of the surface of the glass corresponds to the logarithm of its viscosity (9 to 9.1 Pa s) and in the case of most types of glass, it takes place within the temperature range of 650 to 750 °C.

It is held that there arises a redundant pressure on the gas inside the cavity. So the beginning of the enclosure must depend on the viscosity at which the process of softening starts under pressure, i.e. the starting point of deformation is at about 11 Pa s, and with most of the types of glass takes place within the temperature range of 580 to 630 °C.

2.2 Mathematical model of heat transfer in a glass granulate layer

Processes of thermal field formation in a layer of glass granulate will be dealt with in this section. It is known that glass is a material which is partially transparent to thermal radiation and in it, there forms a thermal field as a consequence of the joint radiation and thermal conductivity. This is described by help of an equation for transfer of energy:

$$\varrho\, C_V \frac{\mathrm{d}T}{\mathrm{d}\tau} \equiv \operatorname{div}(\lambda\, \operatorname{grad} T) - \operatorname{div} q_R \qquad (1)$$

where the first term of the right part describes the transfer of energy due to thermal conductivity and the second term describes the transfer of energy due to thermal radiation. From this, it can be seen that finding a thermal field even in the case of one-direction heat transfer in an absorption - radiating environment is in accordance with a solution to a nonlinear integrodifferential equation. This is because T is contained in the term which determines the heat transfer with a thermal conductivity of the first class and is also contained in the term which determines the transfer by help of radiation – the fourth class.

The solution to this problem has been dealt with in many articles and monographs of which [3] is probably the most credible one.

In our case, the proposed mathematical solution to the problem of a layer of glass granulate will be as follows. The nonstationary thermal distribution is found from the solution to the energy transfer equation:

$$\varrho\, C_p(T) \frac{\partial T}{\partial \tau} = \frac{\partial}{\partial x}\left[\lambda(T) \frac{\partial T}{\partial x} - 2\pi \int \mathrm{d}\nu \int_0^1 (I_\nu^+(\mu, x, \tau) - I_\nu^-(\mu, x, \tau))\right] \mu\, \mathrm{d}\mu \qquad (2)$$

where ν is the frequency of radiation, $\mu = \cos\varphi$ the direction of the radiation, x the co-ordinate of the perpendicular layer of the tile, and τ the time.

The radiation flow is established by help of an equation for spectral intensity of the radiation forward (+) and backward (−):

$$\mu \frac{\partial I_\nu^+(\mu, x, \tau)}{\partial x} + K_{\nu,T}\left[I_\nu^+(\mu, x, \tau) - n_\nu^2 I_{b,\nu}(T)\right] = 0, \qquad (3)$$

$$\mu \frac{\partial I_\nu^-(\mu, x, \tau)}{\partial x} - K_{\nu,T}\left[I_\nu^-(\mu, x, \tau) - n_\nu^2 I_{b,\nu}(T)\right] = 0 \qquad (4)$$

where $I_{b,\nu}(T)$ is the intensity of black body radiation, $K_{\nu,T}$ the spectral-thermal dependence of the absorption coefficient of the glass granulation product, and n_ν is the spectral dependence of the refractive index.

The limit conditions for equations (3 and 4) in the case of an ideal contact with nontransparent boundaries (bottom of the mould) are:

$$I_\nu^-(L, \mu, \tau) = n_\nu^2 I_{b,\nu}(T_2)(1 - R_{2,\nu(\mu)}) + K_2 R_{2,\nu(\mu)} I_\nu^+(L, \mu, \tau) + 2(1 - K_2) \int_0^1 R_{2,\nu(\mu)} I_\nu^+(L, \mu, \tau)\, \mu\, \mathrm{d}\mu \qquad (5)$$

where L is the thickness of the layer of the glass granulation product, $R_{2,\nu(\mu)}$ the directional-spectral reflectivity, and K_2 the degree of diffusibility of the boundary.

For the upper boundary of the glass granulate layer separated from the heater by a diathermic gap, the conditions for the balance of the radiation flow are added:

$$I_\nu^+(0, \mu, \tau) = R_\nu I_\nu^-(0, \mu, \tau) + n_\nu^2 (1 - R_\nu) I_\nu^+(x, \mu', \tau), \qquad (6)$$

$$I_\nu^-(x, \mu', \tau) \equiv R_\nu I_\nu^+(x, \mu, \tau) + \frac{1}{n_\nu^2}(1 - R_\nu) I_\nu^-(0, \mu, \tau), \qquad (7)$$

$$I_\nu^+(x_1, \mu', \tau) \equiv n_\nu^2 I_{b,\nu}(T_1)(1 - R_{1,\nu(\mu')}) + K_1 R_{1,\nu(\mu')}, \qquad (8)$$

$$I_\nu^-(x_1, \mu', \tau) \equiv 2(1 - K_1) \int_0^1 R_{1,\nu(\mu')} I_\nu^-(x_1, \mu', \tau)\, \mu'\, \mathrm{d}\mu' \qquad (9)$$

where in connection with the Snell law:

$$\mu'^2 = 1 - n_\nu^2 (1 - \mu^2) \qquad (10)$$

for $\mu > \mu_h = \sqrt{1 - 1/n_0^2}$.

For $\mu < \mu_h$ the equations 6 to 9 look as follows:

$$I_\nu^+(x, \mu, \tau) = I_\nu^-(x, \mu, \tau) \qquad (11)$$

for $x = 0, L$.

The addition mentioned is exact for a plane of a layer of clearly transparent material which in our case applies virtually ideally since the dimensions of the product are $(400 \times 400)\ \mathrm{mm}^2$ and its thickness is 10 to 15 mm.

In solving the given problem, the substantial influence of the character of the reflection on the boundaries (mirror reflection, diffuse reflection, mirror-diffuse reflection), on the dynamics of the forming of the thermal field and especially on the thermal gradients of the quantities was taken into consideration.

2.3 Mathematical model of heat transfer on the gas bubble boundary

Due to our special interest in the character of the thermal distribution on the boundary of the gas bubble

which is formed of dust particles and is diffusely permeable, we will use a model of flat layer for it. In the case of a characteristic diameter of the bubble of 5 to 8 mm, the coat of the bubble will be 0.05 to 0.1 mm thick. For an analysis of the physical process in the first approximation, this presumption is well proven.

For the coat made of the dust particles, it is absolutely necessary to create conditions for the determination of the normalized intensity values forwards and backwards, as on the inner boundary which is found in the layer of the optical material:

$$I_v^- (x^-, d) = (1 - R_{d,1})\, 2 \int_0^1 I_v^- (x_2, \mu')\, \mu'\, d\mu' + R_{d,1}\, 2 \int_0^1 I_v^+ (x', \mu')\, \mu'\, d\mu' , \quad (12)$$

$$I_v^+ (x^+, d) = (1 - R_{d,2})\, 2 \int_0^1 I_v^+ (x_1, \mu')\, \mu'\, d\mu' + R_{d,2}\, 2 \int_0^1 I_v^- (x_2, \mu')\, \mu'\, d\mu' . \quad (13)$$

For two-way spectral reflection ability of the rays hitting the envelope, for example from the side of the glass layer:

$$\varrho_v''(\mu, \theta, \mu_n, \theta_n) = \frac{1 - K}{\pi} R_{v,d,1} + \frac{K}{\mu_n} R_v(\mu_n)\, \delta (\mu_1 - \mu_n)\, \delta (\theta + \pi - \theta_n) \quad (14)$$

and for two-way permeability of the envelope:

$$\in''(\mu_2, \theta, \mu_n, \theta_n) = \frac{n_2^2}{n_1^2} \left[\frac{K}{\mu_n} \delta (\mu_1 - \mu_n) \cdot \delta (\theta + \pi - \theta_n) - \varrho''(\mu_1', \theta, \mu_n, \theta_n) \right] + (1 - K)(1 - R_{v,d,1}) \quad (15)$$

where K, the coefficient of diffusion, varies from 0 to 1.

The symbols of the other variables are completely identical with the ones in [5 and 6].

2.4 Results of calculation

A detailed examination by help of mathematical modelling made it possible to discover the phenomenon of non-monotonousness and inversion of thermal distribution in the surroundings of the diffusely permeable boundary which is preserved even in the stationary mode (figure 2). In the process of onesided linear heating from room temperature to 1000 K, at the moment of maximum thermal drop, the amplitude of non-monotonousness of the thermal gradient – in the case of small optical thickness – can attain up to 100 K. Table 1 shows dependence of maximum amplitudes of inversions (A_1) according to optical thickness ($D = k\,d$) in a two-layer system with an inner diffuse boundary at the temperatures of the boundaries of 1500 and 300 K. Depending on the refraction indicator, the amplitude of inversion can amount to tens of degrees and as the refraction indicator increases, it attains maximum in the case of high values for optical thickness.

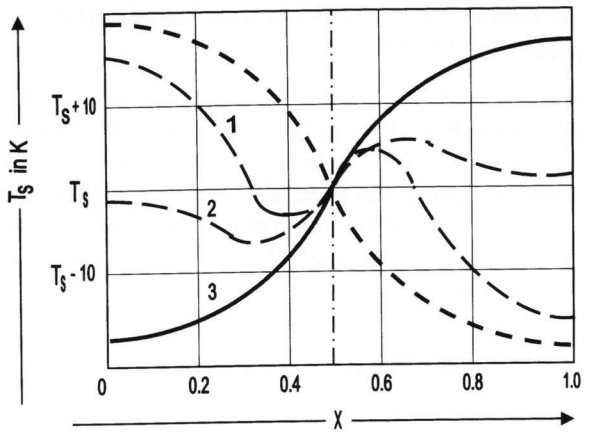

Figure 2. Non-monotonous and inverse temperature distribution in the presence of an inner diffusely permeable boundary representing a plane layer of the optical environment. Curves 1, 2 and 3: temperature distributions for non-dimensional optical thicknesses 1.0, 0.5 and 0.05; –·–·–: inner diffusely permeable boundary, – – –: normal temperature distribution without inner boundary.

Table 1. Maximum amplitudes of the inversion – the calculation results

n	1.01	1.05	1.1	1.2	1.35	1.5	1.75	2.0
$D = k\,d$	0.03	0.05	0.07	0.08	0.09	0.1	0.1	0.11
A_1, K	17.7	41.3	54.6	68.2	47	34	23.1	15.2

As far as the thermal conductivity is concerned, the coat of the cavity, formed of particles which are low-dispersive, represents a layer whose thermal conductivity coefficient is different from that of the main environment. It was established that the thermal conductivity coefficient decreases along with the decrease in the granularity of the material and also if the gaps between the particles are reduced with the volume of the solid substance remaining the same. In our case, this corresponds to the sealing of the surface of the coat of the bubble in the process of expansion when the gas is heated. The term of the effective thermal conductivity of the gas gap is determined by the following relation [6]:

$$\lambda_{\text{eff}} = \frac{S}{6} C_V \varrho u L \tag{16}$$

where u is the average velocity of the gas molecules, S the coefficient of accommodation; ϱ the density, C_V the heat capacity, and L the distance between the grain particles.

It was already established by G. Hengst, a German scientist, that a thermal jump results in the layer of the gas, if the distance between the particles becomes smaller than the distance between the particles of the freely moving gas molecules (see in [6] pp. 307 and 315). This is due to a more complicated movement of the molecules found near the wall. For example, according to [4], for air the coefficient of thermal jump can be 1.6 and for CO_2 it can be 1.1.

Therefore, in the case of heat transfer solely by way of thermal conductivity, a thermal jump also takes place on the coat of the bubble composed of dust particles and this thermal jump is capable of melting the particles on the surface fast and of forming an enclosed cavity [4].

The basic types of glass have the zone of high transparency for heat radiation, i.e. low values of the thermal conductivity coefficient, up to the wavelengths of 4 to 5 μm. Using Vin's relation, we can immediately see that at a temperature of 400 to 450 °C, the heat transfer by way of radiation and by way of thermal conductivity is comparable. Moreover at temperatures higher than 700 °C, the radiation prevails, and in both respects in most cases, there arise conditions for a thermal jump on the coat of the bubble.

2.5 Physical interpretation of the results

The inner surface of the bubble, at the initial stage of its forming, can be imagined as an unbroken surface composed of low-dispersive spherical particles of a diameter < 0.05 mm (figure 3). A thin layer of such particles is an ideal diffuser for the radiation flow falling on it. The examination of the intensity of the radiation both in the direct (I_v^+) and in the indirect (I_v^-) direction shows that the radiation flow diffusely radiates into the inner space of the bubble (V). The radiation of the inner layer (I_{pa}) is also diffuse. In this way, an intensive absorption of both its own radiation and the diffused radiation coming from the passing radiation flow takes place on the inner surface of the bubble being formed, and conditions for a local increase in temperature depending on the surrounding environment composed of large granules of the glass-silicate product are created in the inner space of the bubble. Besides that, a considerable part of the radiation falling on the half-transparent layer is absorbed immediately due to the diffusion. In other words, the bubble being formed in the inner layers of the semi-finished

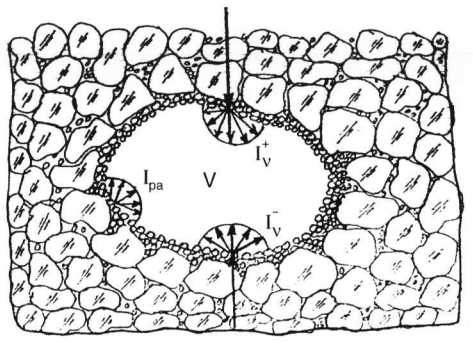

Figure 3. Overheating of the inner cavity due to diffuse distribution of the thermal flux radiation.

product represents a local point with a higher absorption coefficient leading to a local rise in temperature.

We can roughly get the idea of the picture being formed by visualizing that there are local areas originating in the inner layers of the semi-finished product whose degree of blackness is almost equal to 1 and the radiation passing through them is totally absorbed, which increases their temperature. Thus, the semi-finished product represents a layer of a partially transparent granulated material containing totally black little bodies distributed chaotically.

It should be observed that the phenomenon of inversion was first discovered by this author together with Aronov and Marchenko in theory [4] and then experimentally [5] in observing radiation-conductive heat transfer in the process of growing optical crystals.

2.6 Role of chemical reactions

In the process of bubble formation during thermal processing of glass-silicate products the chemical reactions taking place also play an important role. When using glass industry wastes as the source raw material for the making of glass-silicate slabs, the possibility that sodium, calcium and magnesium carbonate and also the bicarbonates $Na_2Ca(CO_3)$ and $CaMg(CO_3)$ used in glassworks may fall into the semi-finished product cannot be ruled out. Their occurrence in the original mixture of these materials in the presence of SiO_2 leads to the formation of bubbles during thermal processing where CO_2 is liberated in the course of the reactions given in table 2. The temperature at which the reaction takes place is shown in the right column.

Here, we can easily identify that the temperature zones of the maximum liberation of CO_2 and of the maximum radiation absorption (figure 4) are identical. Taking into account the spectrum of radiation, we obtain the following temperature zones: 300 to 440 °C; 690 to 880 °C and 1120 to 1200 °C. This creates supplementary conditions for the local overheating of bubbles.

Table 2. Various chemical reactions occurring in the process of bubble formation within temperature zones of maximum CO_2 liberation

reaction	temperature in °C
$CaNa_2(CO_3)_2 + 2SiO_2 \rightleftharpoons Na_2SiO_3 + CaSiO_3 + 2CO_2$	600 to 830
$MgCO_3 \rightarrow MgO + CO_2$	300
$MgNa_2(CO_3)_2 + 2SiO_2 \rightarrow MgSiO_3 + Na_2SiO_3 + 2CO_2$	340 to 620
$MgCO_3 + SiO_2 \rightarrow MgSiO_3 + CO_2$	450 to 645
$Na_2CO_3 + SiO_2 \rightarrow Na_2SiO_3 + CO_2$	from 380
$CaCO_3 \rightarrow CaO + CO_2$	from 420
$CaCO_3 + SiO_2 \rightarrow CaSiO_3 + CO_2$	600 to 920

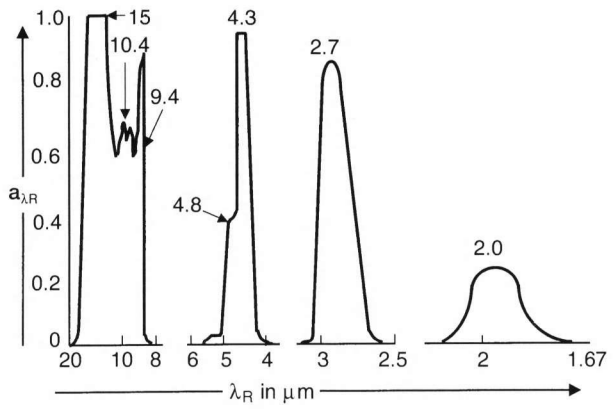

Figure 4. Spectrum of CO_2 absorption versus wavelength of radiation λ_R.

3. Experimental part

3.1 Description of gas bubble forming processes

Various bubbles can be well seen in figure 5. The inner surface of all of them is smooth like a mirror. This means that its melting started before the melting of the glass granulate surrounding the cavity and took place at higher temperatures than the ones which are in the immediate proximity of the bubble. Besides that, remnants of CaO and MgO were discovered in many bubbles which confirms the hypothesis about the course of the reactions mentioned in section 2.6.

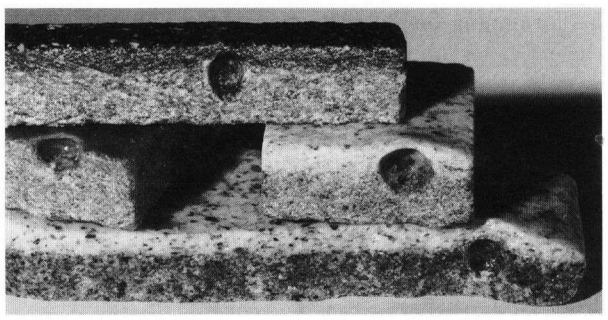

Figure 5. Typical gas bubbles in glass-silicate tiles.

It is highly probable that the result of the reactions i.e. the decomposition of carbonates, is the basis for the formation of bubbles because CO_2 creates ideal conditions for a local overheating in a bubble and subsequently, during the enclosing of the cavity, even larger grains of the glass granulate can play their role.

When types of glass with a lower Littleton temperature were used in the experiments, no CaO residues were found in the bubbles. This is due to the fact that in this case the maximum temperature of the thermal processing was 880 °C at the surface and not higher than 820 to 830 °C in the inner layers of the semi-finished product. The maximum rate of decomposition of $CaCO_3$ corresponds with a temperature of 915 °C in those cases where the intensive decomposition of $MgCO_3$ takes place within the temperature range of 350 to 470 °C, i.e. before the inner side of the bubble starts to melt on the surface, and the resulting gas is able to emerge from the inner layers into the free space. An increase in the maximum temperature up to 960 to 970 °C leads to a sharp increase in the number of bubbles. Many of them are able to emerge on the surface because the viscosity of the upper melted layer decreases by 1.5 to 2 orders due to the increase in temperature.

Figures 6a to d show this process in the form of a diagram. At the initial stage (figure 6a), starting from the top, the semi-finished product is heated by help of a heat flux q. The product is composed of two layers: the upper layer contains colour glass granulate sized according to the required design and the bottom layer fine glass granulate with sand. At this stage, the diffusing gas can freely penetrate into the space of the furnace through the gaps between the granules. Due to a low value of the thermal conductivity coefficient of the poured-in material (usually $\lambda < 1.5$ W/(m·K) in the direction through the thickness of the semi-finished product, a high thermal gradient is established during the heating. At the stage shown in figure 6b, the surface melting and melting away of the upper layer take place at the time when in the bottom layer the reactions liberating CO_2 start to take place, and a loose structure with a large number of cavities is formed. In further heating (figure 6c), the bubbles join to form larger ones and the structure of the bottom layer is strengthened by sintering and melting the contained glass granulation product. When the maximum temperature on the surface that is processed thermally is attained, the heating is terminated (figure 6d). But the process of evening the thermal gradient continues. The bubbles formed are rising to the surface but due to the high viscosity of the melted glass, many bubbles do not succeed in reaching the surface and remain in the inner layers, which weakens the inner structure of the material. Uneven areas and bulges are formed on the surface as a consequence of the fact that gas bubbles are found in the inner layers.

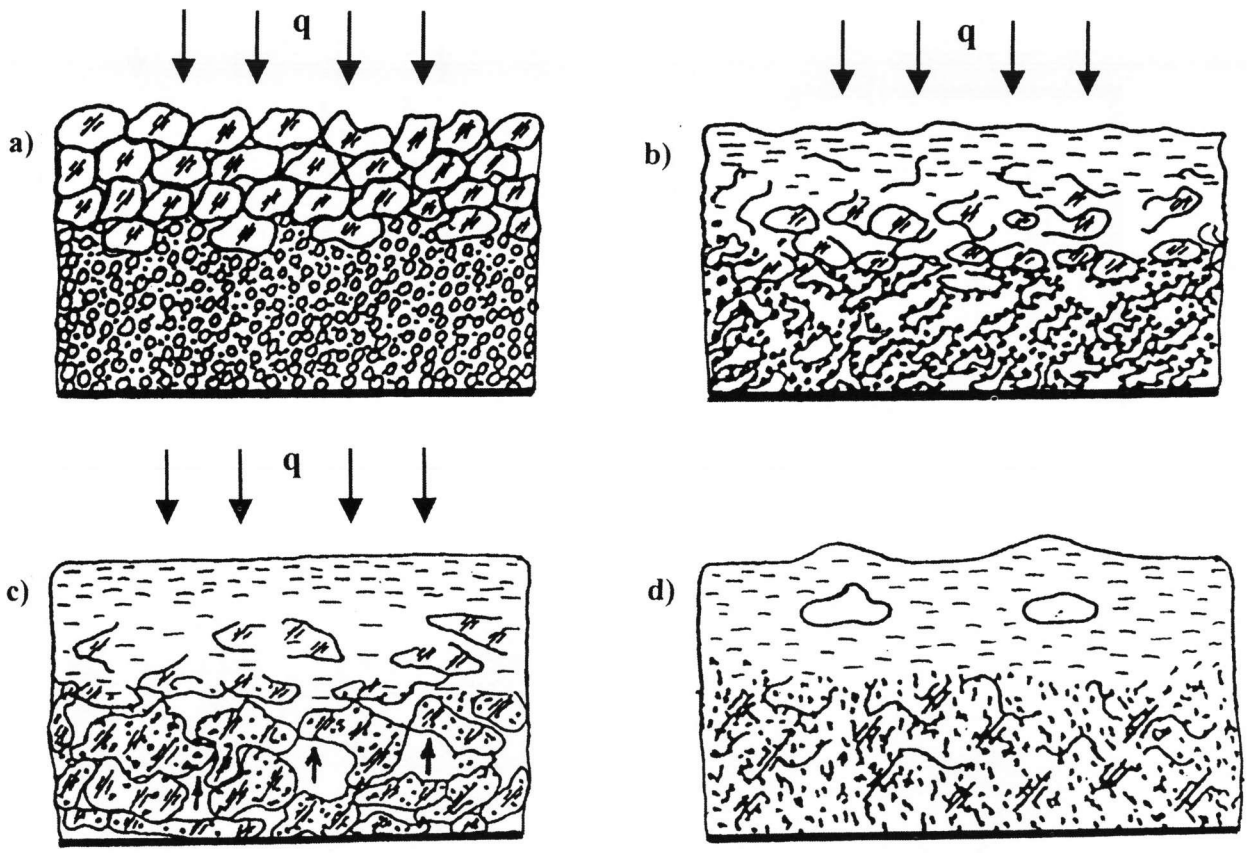

Figures 6a to d. Formation and floating of gas bubbles formed as a result of chemical reaction; a), b), c) and d) successive stages of bubble formation.

3.2 Experimental verification of temperature field inversion

The experimental verification of the phenomenon of thermal field inversion took place in a special measuring cell (figure 7) in the following way:

Between the heater (4) and the cooler (3) with blackened surface, a two-layer sample (1) was spread. The radiation of both sides of the sample was directed by help of rotary mirrors (6) which ensure the absolute similarity of the optical channels. The whole construction was put in a thermally insulated body (5) and the holders holding the sample (2) were made of heat-resistant material with a thermal expansivion coefficient lower than that of glass, which ensures the density of the contact in the middle layer during the process of heating the sample. For measuring the thermal gradient, a special highly sensitive UK-pyrometer (7) with a resolution ability of 0.2 K and a black body model up to temperature 1900 K were used.

The method used in the experiment was as follows: Two discs of quartz glass of a diameter of 120 mm and a thickness of 10 mm, each with polished surface, were clamped tightly to each other and placed in the measuring cell. In the process of heating, the following values were measured: temperature of the heater, temperature of the surface of the sample facing the heater and the decrease in temperature between the surfaces. In all thermal zones, the temperature of the surface facing the heater is higher than that of the surface facing the cooler – a positive gradient. In the case of temperatures higher than 1100 K, some increases in the thermal gradient are conditioned by the spectral composition of the radiation emitted by the heater and by the spectrum of the absorption of the samples tested.

In the following series of experiments, the sides of the samples which formed the inner boundary were ground and had micro-unevenness approximately of the size of 1 to 5 μm, i.e. an inner diffuser for identical wavelengths of the radiation emitted by the heater was made. At low temperatures when the molecular thermal conductivity of the glass participates in the forming of thermal distribution (maximum energy is let through by the heater in the nontransparent area), the thermal gradient is also positive – curve 2 shown in figure 8.

Starting from 680 K at which temperature the radiation begins to play a comparable and, further on, a dominating role in forming the thermal field, the thermal gradient is visibly dropping and then becomes negative. This essentially confirms the rise of inverse distribution due to the diffusion of radiation on the inner diffusely permeable boundary.

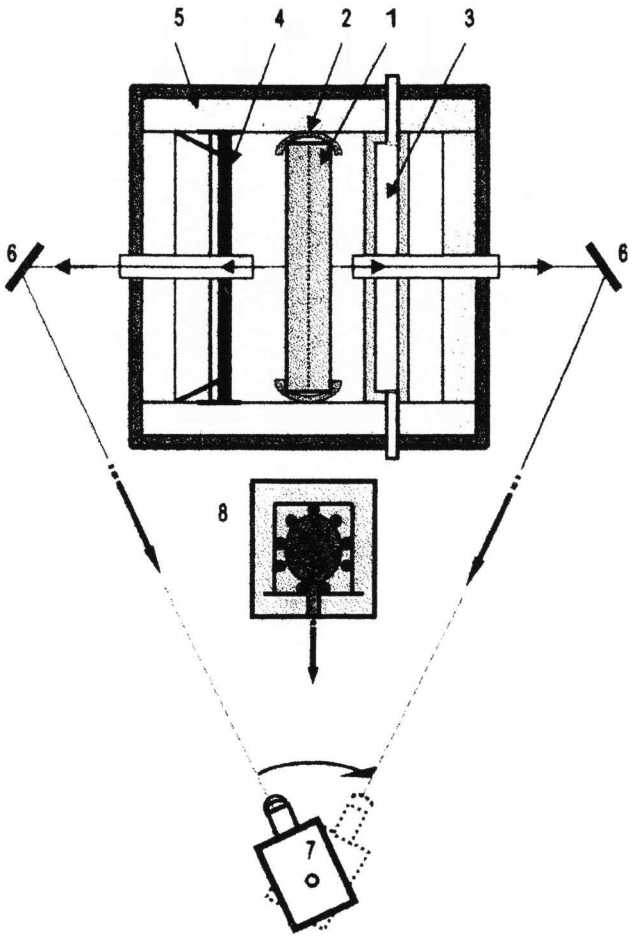

Figure 7. Experimental equipment; 1: sample with inside diffuse-gray surface, 2: holder for sample, 3: cooling element with black or mirror surface, 4: heating element (up to 1920 K) with black surface, 5: experimental box with heat insulation, 6: IR mirrors, 7: IR pyrometer, and 8: model of black body.

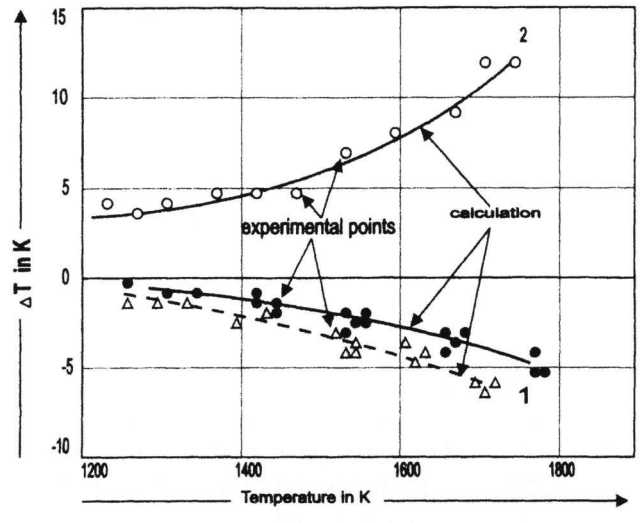

Figure 8. Results of research into temperature field inversion for different surfaces investigated with the equipment shown in figure 7; roughness of surface: (•) 15 to 20 μm, (Δ) 3 to 5 μm, (○) mirror surface; curve 1: diffuse-gray inside surface, curve 2: mirror inside surface.

An absolutely analogous phenomenon occurs on the coat of the bubble formed of the dust glass particles.

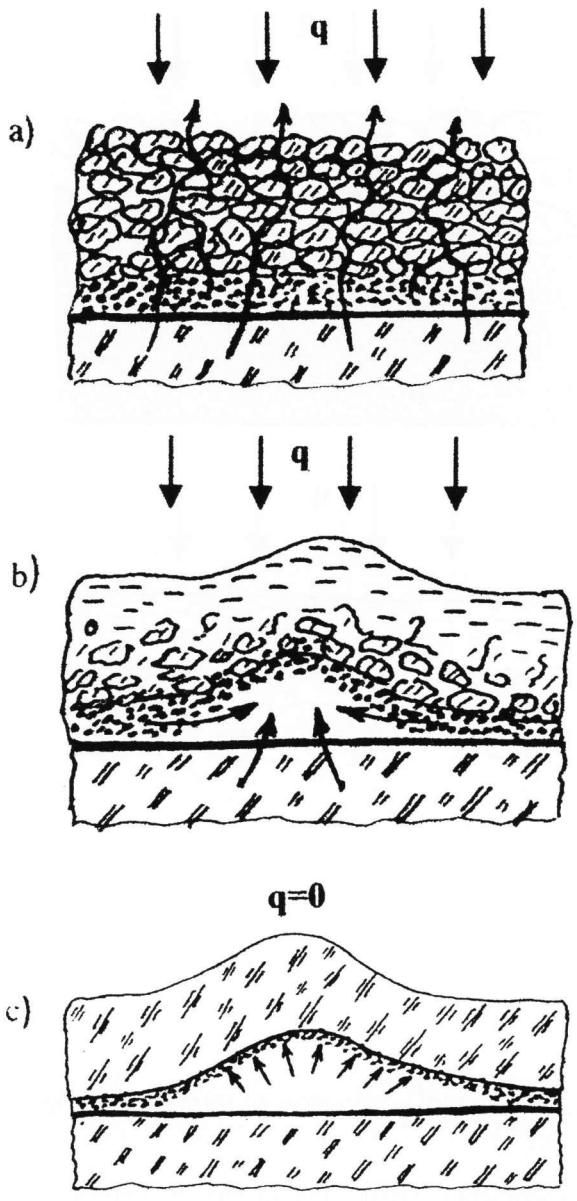

Figures 9a to c. Mechanism of super-bubble formation; a) during heating process (q) escape gases pass through glass granulate particles; b) upper layer is melted, but gases continue to escape in bottom layer and from the ceramic form; c) upper layer is solidified ($q = 0$), but gases between bottom layer and ceramic form continue to increase.

3.3 Formation of super-bubbles

There are also cases in the production of glass-silicate slabs where huge bubbles are formed, which we called super-bubbles, sometimes having diameter of 10 to 12 cm with slab dimensions of (40 × 40) cm^2. The diagram of this process is shown in figures 9a to c.

In the production of single-layer slabs, the layer of glass granulate is poured into a ceramic mould whose surface is covered with a layer of kaolin. During the heating at the initial stage (figure 9a), the gases found in the layer of the glass granulate, and of the kaolin and in the mould, where they expand, have the possibility to escape into the space of the furnace through half of the semi-finished product. According to the degree to which

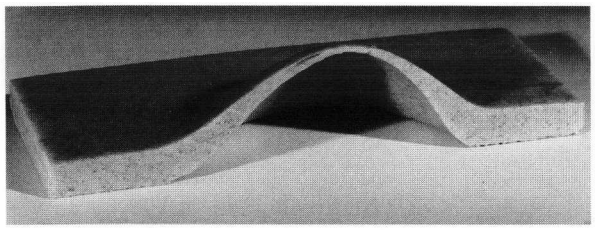

Figure 10. Super-bubble formed in thermal processing of a single-layer semi-finished product.

the glass granulation product is melted (in the direction from the top downwards), the expanding bubbles start to gather in the gap between the bottom of the mould and the bottom of the slab (figure 9b). The continuing process of heating the whole semi-finished product and the bottom of the mould leads to gathering of the liberated gases under the layer of the melted glass granulate and to their movement in horizontal direction. This is because due to the high viscosity of the melted layer, the gases cannot escape through it to the space of the furnace. Their joining at one or several points consequently leads to the formation of one large super-bubble which, under the pressure of the gases gathered, bulges the semi-finished product (figure 9c), forming a shape of a hill.

The result of the super-bubble formation can be well seen in figure 10. Here, it must be observed that the formation of the super-bubbles is definitely related to the rate at which the semifinished product is heated, i.e. to the value of the thermal gradient in the direction through the thickness of the semifinished product and to the porosity of the bottom of the mould, i.e. to the quantity of gas which is able to escape out of the mould during its heating.

4. Conclusion

The examined mechanisms of the bubble formation taking place during thermal processing of glass-silicate slabs, made according to the granule-powder technology, are the main cause for defective products under industrial conditions.

Most unfavourable is the situation where a chemical reaction liberating CO_2 occurs simultaneously with the gathering of dust particles. In this case, radiation-conductive heat transfer processes in the inner layers are able to considerably preheat the gas found inside the bubble formed and to form an enclosed coat of the cavity.

The phenomena of the thermal field inversion occurring on a layer diffusely permeable to heat radiation as described in this work have a general character and can be the cause of bubble formation in thermal processing of other materials where low-dispersive size fractions of these materials are used.

In the publications to follow, examination of all mechanisms of the formation of various kinds of bubbles under the conditions of thermal processing of granule-powder materials will be carried out.

5. Nomenclature

5.1 Symbols

A_I	maximum amplitude of inversion
$a_{\lambda R}$	absorption factor
C_V	heat capacity of constant volume
C_p	heat capacity at constant pressure
d	thickness of a melted layer inside the bubble
D	optical thickness
I_P	Planck's function of radiation
I_{pa}	diffuse emission of glass dust particles
$I_\nu^{-,+}$	spectral intensity of radiation
$I_{b,\nu}$	intensity of black body radiation
k	integral absorption coefficient
K	coefficient of diffusion
$K_{\nu,T}$	spectral-thermal absorption coefficient
$K_{1,2}$	coefficient of diffusion of boundary 1 and 2
l	distance between grain particles in equation (9)
L	thickness of the layer of the glass granulation product
n	refractive index
n_ν	spectral refractive index
$n_{1,2}$	refractive index of boundary 1 and 2
q	heat flux
q_R	radiation flux
Q	total heat flux
R_ν	spectral reflectivity
$R_{\nu(\mu)}$	directional spectral reflectivity
$R_{d,1}$	reflectivity of nontransparent boundary 1
$R_{d,2}$	reflectivity of nontransparent boundary 2
$R_{\nu,d,1}$	directional spectral reflectivity of boundary 1
$R_{\nu,d,2}$	directional spectral reflectivity of boundary 2
$R_{1,\nu(\mu)}$	spectral reflectivity of boundary 1 in direction μ
$R_{2,\nu(\mu)}$	spectral reflectivity of boundary 2 in direction μ
S	coefficient of accommodation
T	temperature
$T_{1,2}$	temperature of boundary 1 and 2
T_S	temperature in the middle section of the optical layer
u	average velocity of gas molecules
V	volume of gas bubble
x	coordinate
x_1	coordinate of boundary 1
x_2	coordinate of boundary 2
X	non-dimensional thickness
δ	optical density
θ	azimuth of angle for falling beam
θ_n	azimuth of angle for direction n
λ	thermal conductivity
λ_{eff}	effective thermal conductivity
λ_R	wavelength of radiation
μ	direction of radiation
μ_n	cosine of angle in direction n
μ_h	cosine of angle of fully internal reflection
$\mu_{1,2}$	cosine of angle on boundary 1 and 2, accordingly
ν	frequency
$\nu_{(\mu)}$	frequency of radiation in direction μ
π	constant
ϱ	density
ϱ_ν	spectral density
τ	time

5.2 Superscripts

+	forward
-	backward
′	direction for inside beam
″	two-directional

5.3 Subscripts

b,ν	spectral intensity of black body
c	conductivity
d,1	diffusely reflecting surface 1
d,2	diffusely reflecting surface 2
eff	effective
h	direction for beam of fully internal reflection
I	inversion
n	perpendicular direction
P	Planck's function
p	pressure
pa	particle
R	reflected radiation
T	temperature
V	volumetric
1	opaque boundary 1
2	opaque boundary 2
0	middle line
λ	wavelength
ν	spectral
$\nu_{(\mu)}$	spectral in direction μ

Contact:

Prof. J. Linhart, Dr. Sc.
PRT - Progressive Technologies s.r.o.
Benesovska 26
10100 Prague 10
Czech Republic
E-mail: prt@progtech.cz

6. References

[1] Lingart, Y.: Imitation natural material tiling using waste glass. Glass Technol. **39** (1998) no. 2, p. 42–43.
[2] Lingart, Y.; Lingart, M.; Lingart, S.: Method for making glass silicate tiles. USA pat. 5, 900, 202. May 4, 1999.
[3] Siegel, R.; Howell, J. R.: Thermal radiation heat transfer. New York et al.: McGraw-Hill, 1972.
[4] Aronov, B.; Lingart, Y.; Marchenko, N.: Inversion of the temperature field in sapphire. Thermal Physics of High Temperatures **XXIVI** (1987) no. 1, p. 191–193. (Orig. Russ.)
[5] Aronov, B.; Lingart, Y.; Marchenko, N.: Inversion of the temperature field of semitransparent layer. Thermal Physics of High Temperatures **XXVII** (1989) no. 4, p. 737–744. (Orig. Russ.)
[6] Missenard, A.: Conductivité thermique des solides liquides, gaz et de leurs mélanges. Paris: Eyrolles, 1965. p. 165–179.
[7] Lingart, Y.; Petrov, V.: Measurement of surface temperature of optical semitransparent materials. In: Proc. Temperature measurement, Prague, 1981. p. 105–118.

Note: In references [1, 2, 4, 5 and 7] the author's name is spelt according to a transcription from Russian to English.

E402P004